Available online at www.sciencedirect.com
ScienceDirect
Journal of Molecular Catalysis A: Chemical 282 (2008) 52–61
JOURNAL OF MOLECULAR CATALYSIS A: CHEMICAL
www.elsevier.com/locate/molcata

LSCF and Fe_2O_3/LSCF powders: Interaction with methanol

Alessandro Galenda, Marta Maria Natile, Antonella Glisenti *

Dipartimento di Scienze Chimiche, Università di Padova, Via Marzolo 1, I-35131 Padova, Italy

Received 5 July 2007; received in revised form 13 November 2007; accepted 14 November 2007
Available online 26 November 2007

Abstract

This work focalizes on a nanosized $La_{0.6}Sr_{0.4}Co_{0.8}Fe_{0.2}O_{3-\delta}$ (LSCF) perovskite and Fe_2O_3/LSCF nanocomposites. The nanosized LSCF perovskite is obtained by Pechini method and treated at 1173 K; nanocomposite Fe_2O_3/LSCF powder samples (Fe_2O_3/LSCF = 1:9 and 1:1 wt.) are obtained by wet impregnation.

The reactivity of the obtained samples with respect to pure methanol and to a 1 M aqueous solution of methanol, is investigated by means of IR Spectroscopy and Quadrupole Mass Spectrometry (QMS). In presence of pure methanol the main reaction is methanol decomposition with the formation of CO and H_2. The activity with respect to this reaction starts to be observed at 573 K both for the LSCF perovskite and for the Fe_2O_3/LSCF nanocomposites and shows an irregular trend as a function of temperature. Steam-reforming reaction is evident at $T \geq 623$ K when a 1 M solution of methanol is used. The reactivity with respect to methanol and to the 1 M solution of methanol was also investigated as a function of time: only at 673 K the methanol decomposition starts immediately; the waiting time changes as a function of temperature, sample composition and reactive mixture. The steam reforming reaction, in contrast, begins immediately.

Keywords: Perovskite; Methanol oxidation; LSCF; Oxide; Nanomaterials

1. Introduction

Attaining sustainable development is one of the greatest challenges we face today, a challenge that can only be met by responsibly developing and using technologies. Fuel cells offer an opportunity for innovation; as a matter of fact, today's innovations in fuel cell technology are focussing scientific efforts: innovative solutions can be an important competitive plus. Fuel cells are not just laboratory curiosities but still much work needs to be done to optimise the fuel cell systems.

In this respect perovskite-type oxides show interesting properties such as electronic/ionic conductivity, catalytic activity, etc. [1] that make them promising in several fields. Among these, the so-called Intermediate Temperature SOFCs (IT-SOFCs $T \sim 800$ K) is one [2].

This contribution is part of a comprehensive work aimed to the investigation of LSCF-based materials [3]. Perovskite-type complex oxides of $La_{1-x}Sr_xCo_{1-y}Fe_yO_{3-\delta}$ [4–6] composition have attracted growing attention because of their superior mixed electronic–ionic conduction properties. Moreover, their long-term stability of structure and properties at elevated temperatures has to be considered. $La_{0.6}Sr_{0.4}Co_{0.8}Fe_{0.2}O_{3-\delta}$, in particular, exhibits superior sinterability and good mixed electronic–ionic conduction properties [7,8]. Reactivity toward alcohols, however, needs to be investigated. In this paper the interaction with methanol is considered. Methanol is an important probe molecule being an intermediate in several oxidation reactions; moreover, it is a simple organic molecule characterized by a significant acidity. It is noteworthy that methanol can also be a promising fuel for fuel cells. In addition to the $La_{0.6}Sr_{0.4}Co_{0.8}Fe_{0.2}O_{3-\delta}$ two new materials obtained by depositing iron oxide on the perovskite surface (Fe_2O_3/LSCF = 1:9 and 1:1 wt.) are investigated. As a matter of fact, iron oxide is known to favor methanol oxidation [9] and could improve the electronic conductivity of the perovskite.

The LSCF was obtained by Pechini method which allows to prepare homogeneous perovskite powders in an easy and reproducible [10–12] way; the supported samples were prepared by wet impregnation [13,14]. The interaction with methanol was studied (at several temperatures from room temperature to 673 K) both in absence and in presence of steam. The steam pres-

* Corresponding author. Tel.: +39 0498275196; fax: +39 0498275161.
E-mail address: antonella.glisenti@unipd.it (A. Glisenti).

1381-1169/$ – see front matter © 2007 Elsevier B.V. All rights reserved.
doi:10.1016/j.molcata.2007.11.019

ence, in fact, can strongly influence the reaction products and un-favors carbon formation [15]; moreover, similar operative conditions are used in methanol fed SOFCs. To investigate the obtained products, Quadrupole Mass Spectrometry (QMS) and IR spectroscopy were used. As a matter of fact, QMS furnishes a detailed analysis of the products allowing, in addition, to follow the reaction as a function of time whereas IR spectroscopy is complementary to QMS because by means of this technique the products identification is easier and more precise. The possibility to obtain hydrogen from alcohols was investigated taking into consideration several oxide-based catalysts [16–19]. The reactivity of $La_{0.6}Sr_{0.4}Co_{0.8}Fe_{0.2}O_{3-\delta}$ (LSCF)-based perovskites, in this respect, still needs to be studied.

2. Experimental

2.1. Synthesis

2.1.1. LSCF

The powder was prepared by Pechini method [10–12]. Appropriate amounts of $Co(NO_3)_2{\cdot}6H_2O$ (Acros—99%), $La(NO_3)_3{\cdot}6H_2O$ (Aldrich—99.999%), $Sr(NO_3)_2$ (Carlo Erba—>98%) and $Fe(NO_3)_3{\cdot}9H_2O$ (Janssen—99%) were carefully weighed and dissolved in distilled water in order to obtain $La_{0.6}Sr_{0.4}Co_{0.8}Fe_{0.2}O_{3-\delta}$. Citric acid was added as the complexing agent to the above solution. The amount of citric acid (Acros—99.5%) was such that the ratio of total number of moles of cations to that of citric acid was 1:1. Ethylene glycol (Acros—>99%) was then added (number of moles of ethylene glycol/number of moles of citric acid, 1:1) in order to enhance gelation. The obtained solution was heated at 353 K to remove most of the aqueous solvent and form the gel. Subsequently it was slowly treated at 383 K to remove the remaining solvent and at 673 K to decompose the organic network and the remaining nitrates. By heating at 1173 K for 26 h the perovskite phase $La_{0.6}Sr_{0.4}Co_{0.8}Fe_{0.2}O_{3-\delta}$ is formed.

2.1.2. Fe_2O_3/LSCF

The two Fe_2O_3/LSCF nanocomposite systems (Fe_2O_3/LSCF = 1:9 and 1:1 wt.) were obtained by wet impregnation of LSCF heated at 1173 K for 26 h with aqueous solutions containing increasing quantities of $Fe(NO_3)_3{\bullet}9H_2O$. The obtained suspension was maintained under stirring for 2 days and then kept in rest for 1 day. Water was evaporated in air and the obtained solid was dried at 383 K for 1 h and at 773 K for 5 h (in air).

2.2. Measurements

X-ray Photoelectron Spectroscopy (XPS) measurements were performed using a PerkinElmer PHI 5600 ci spectrometer with a standard Mg Kα source (1253.6 eV) working at 350 W. The working pressure was less than 7×10^{-7} Pa. The spectrometer was calibrated by assuming the binding energy (BE) of the Au $4f_{7/2}$ line to be 84.0 eV with respect to the Fermi level. Extended spectra (survey) were collected (187.85 eV pass energy, 0.4 eV $step^{-1}$, 0.05 s $step^{-1}$). Detailed spectra were recorded for the following regions: C 1s, O 1s, La 3d, Co 2p, Sr 3d and Fe 2p (11.75 eV pass energy, 0.1 eV $step^{-1}$, 0.1 s $step^{-1}$). The standard deviation in the BE values of the XPS line is 0.10 eV. The atomic percentage, after a Shirley-type background subtraction [20], was evaluated by using the PHI sensitivity factors [21]. To take into account charging problems the C 1s peak was considered at 285.0 eV [22] and the peaks BE differences were evaluated.

X-ray Diffraction (XRD) patterns were obtained with a Bruker D8 Advance diffractometer with Bragg-Brentano geometry using a Cu Kα radiation (40 kV, 40 mA, λ = 0.154 nm).

The IR spectra were collected with a Bruker Tensor 27 spectrometer (accumulating 32 scans at a resolution of 1 cm^{-1}).

QMS data were obtained by means of a System Genesys I 200D by European Spectrometry Systems. Background gas contributions to the spectrum were eliminated by subtracting from the spectrum recorded during chemisorption the one obtained just before. Mass spectra assignments were made in reference to the fragmentation patterns; [23,24] moreover, the contributions of the observed species were corrected taking into account the fragmentation patterns of each one and the intensities (partial pressures) of the different masses as a function of temperature were considered. Prior to each experiment, ca. 41 mg of the sample were loaded in the glass reactor. The temperature of the powder was checked by means of a thermocouple inserted into the reactor. Before measurements, the powder was kept in argon flow to eliminate water traces (ca. 2 h).

In each test, vapors of pure methanol or of methanol 1 M solution were carried by an inert gas (argon) from the bubbler to the tubular glass reactor. Then, the reaction products and the un-reacted reagents reached the FTIR and QMS for the analysis. The gas flow was set at 130 cm^3/min by a MKS-mass flow controller. Repeated measures were carried out at each temperature to confirm the observed results. Moreover, at each temperature (from room temperature to 673 K), the reaction was followed as a function of time.

3. Results and discussion

3.1. Characterization

Before the reactivity investigation, the samples were characterized by means of X-ray Diffraction and X-ray Photoelectron Spectroscopy.

Fig. 1 shows the XRD patterns for LSCF treated at 1173 K for 26 h and for the impregnated samples. The LSCF pattern of LSCF, agrees with the presence of the desired perovskite phase; $SrLaCoO_4$ phase and traces of La_2O_3 and Co_3O_4 are also observed [25]. The crystallite size, evaluated by means of X-ray broadening, is estimated at about 80 nm [26]. In the XRD pattern of the supported sample with lower iron content several signals appear while those corresponding to La_2O_3 disappear. The comparison with the JCPDS cards and EXAFS data [3] suggests also the presence of $Sr_{0.4}Fe_{0.6}La_{0.6}Co_{0.4}O_3$ and $SrCO_3$, however the possible reciprocal solubility of the phases has always to be considered. In the sample with higher iron oxide content, the crystallographic disorder increases: contributions due to Fe_2O_3

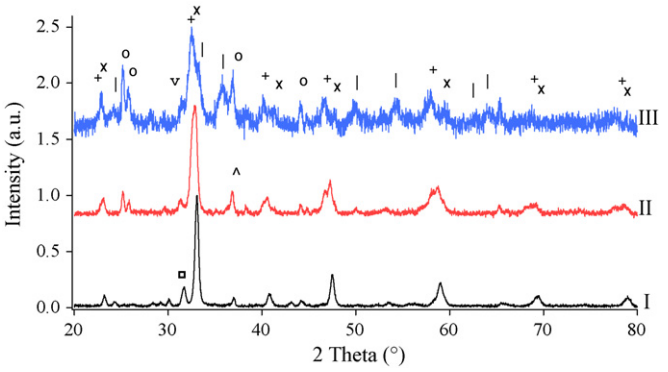

Fig. 1. XRD patterns obtained for the LSCF powder samples (I), and for the Fe_2O_3/LSCF supported samples 1:9 (II) and 1:1 (III). The spectra are normalized with respect to their maximum value. (×) $La_{0.6}Sr_{0.4}Co_{0.8}Fe_{0.2}O_{3-\delta}$, (+) $Sr_{0.4}Fe_{0.6}La_{0.6}Co_{0.4}O_3$, (◯) $SrCO_3$, (^) Co_3O_4, (|) Fe_2O_3, (□) $SrLaCoO_4$ and (v) $SrLaFeO_4$.

and $SrLaFeO_4$ phases appear; several iron rich phases ($Fe_{2.94}O_4$, $Sr_4Fe_3O_{10-x}$ and $FeLaO_3$) as well as $LaCoO_3$ [25] cannot be excluded.

The La 3d peak positions (834.4 and 837.5 eV for La $3d_{5/2}$ and the corresponding shake-up contribution) and shape (Fig. 2) observed for LSCF sample agree with the value reported in literature [27,28]. The Co 2p peak position (Co $2p_{3/2}$ 780.4 eV) and, particularly the absence of evident signals due to the shake-up contributions of Co $2p_{3/2}$ and $2p_{1/2}$ (at about 787 and 805 eV, respectively, Fig. 2) [27,29–33] are indicative of the low spin cobalt Co(III) compounds. Concerning Fe 2p (Fig. 2), the peak position (Fe $2p_{3/2}$ at 711.0 eV) and the shake-up signals (at about 718 eV) suggest the presence of Fe(III) [22]. The Sr 3d peak shape (Fig. 2) is consistent with the presence of more contributions. The fitting procedure reveals three pairs of spin-orbit doublets (at 131.8, 133.5; 132.8, 134.6; 133.8, 135.5 eV, respectively) which indicate that strontium exists in three chemical environments. The spin-orbit doublets at higher BE are ascribable to $SrCO_3$ and [34,35]. The spin-orbit doublet at lower BE agrees with the perovskite phase [29,36] although the presence of strontium suboxide (SrO_{1-x}) cannot be excluded [28,31,37].

The O 1s peak (Fig. 2) shows three contributions corresponding to the perovskite phase (528.7 eV) and hydroxides or carbonate species such as LaOOH or $SrCO_3$ (529.7 and 531.4 eV) [30,38,39]. Accordingly, C 1s peak (Fig. 2) shows, besides the signal due to the adventitious carbon, another contribution at about 289.4 eV corresponding to carbonate species.

Significant differences can be observed in the supported samples and, particularly, in the nanocomposite richer in iron. The La 3d peak shifts toward BE values (834.3 and 838.0 eV for Fe_2O_3/LSCF 1:9, 835.0 and 838.6 eV for Fe_2O_3/LSCF 1:1) characteristics of the lanthanum oxide/hydroxide. The relevant presence of oxides (La_2O_3, Fe_2O_3) is also confirmed by the O 1s signal showing a main contribution around 530 eV.

The Co 2p, Fe 2p and Sr 3d peak shape and positions do not change significantly as a consequence of the iron oxide deposition. In the Sr 3d peak the higher BE contribution decreases significantly.

Table 1
XPS and nominal compositions (atomic%) for LSCF perovskite and for the two Fe_2O_3/LSCF samples

Element	LSCF		Fe_2O_3/LSCF 1:9		Fe_2O_3/LSCF 1:1	
	XPS	Nominal	XPS	Nominal	XPS	Nominal
La	6	14	8	10	6	4
Sr	15	9	8	8	6	4
Co	12	18	8	17	3	8
Fe	4	4	10	10	17	26
O	63	55	66	55	68	58

The comparison between the nominal (obtained by the weighed precursor amounts) and the XPS compositions (Table 1) shows the surface segregation of Sr (which is in agreement with the relevant formation of carbonate species); in the supported samples the more evident result is the low iron atomic percentage that suggests the diffusion of this element inside the support. Moreover, a significant crystallinity decrease is observed in the supported sample richer in iron (Fe_2O_3/LSCF 1:1 wt.) [3] (Table 1).

3.2. Interaction with methanol

3.2.1. LSCF: interaction with methanol

QMS outcomes suggest that the catalytic activity with respect to methanol begins to be evident around 573 K (Fig. 3a); the only observed products are CO and H_2; IR spectra confirm this result (Fig. 4a).

At 573 K the CO and H_2 formation starts only after ca. 420 s and increases slowly aiming to reach a plateau after about 1200 s (Fig. 5).

At 623 K a slight decrease in the catalyst activity is suggested by QMS data (Fig. 5) and confirmed by IR spectra (Fig. 4a). A different behavior is also revealed by the careful comparison with the data obtained at 573 K: CO and H_2 formation starts immediately but decreases with the reaction time (reaching the lower value in 1500–1700 s). In the very first instants of the reaction, however, traces of carbon dioxide are evidenced by QMS. At 673 K, in contrast, the CO and H_2 formation is rather stable with time. The reactivity drop at 623 K and the different behavior observed as a function of time, suggests some consideration concerning the reaction mechanism.

The obtained results suggest that LSCF possesses a catalytic activity with respect to methanol. The formation of CO and H_2 is consistent with the methanol decomposition reaction [15]:

$$CH_3OH \rightleftarrows CO + 2H_2 \quad (1)$$

The initial formation of carbon dioxide observed at $T \geq 623$ K could be ascribed to the following reactions:

$$2CO \rightleftarrows C + CO_2 \quad (2)$$

$$CO + O_P \rightleftarrows CO_2 + O_V \quad (3)$$

with O_P = perovskite oxygen and O_V = oxygen vacancy.

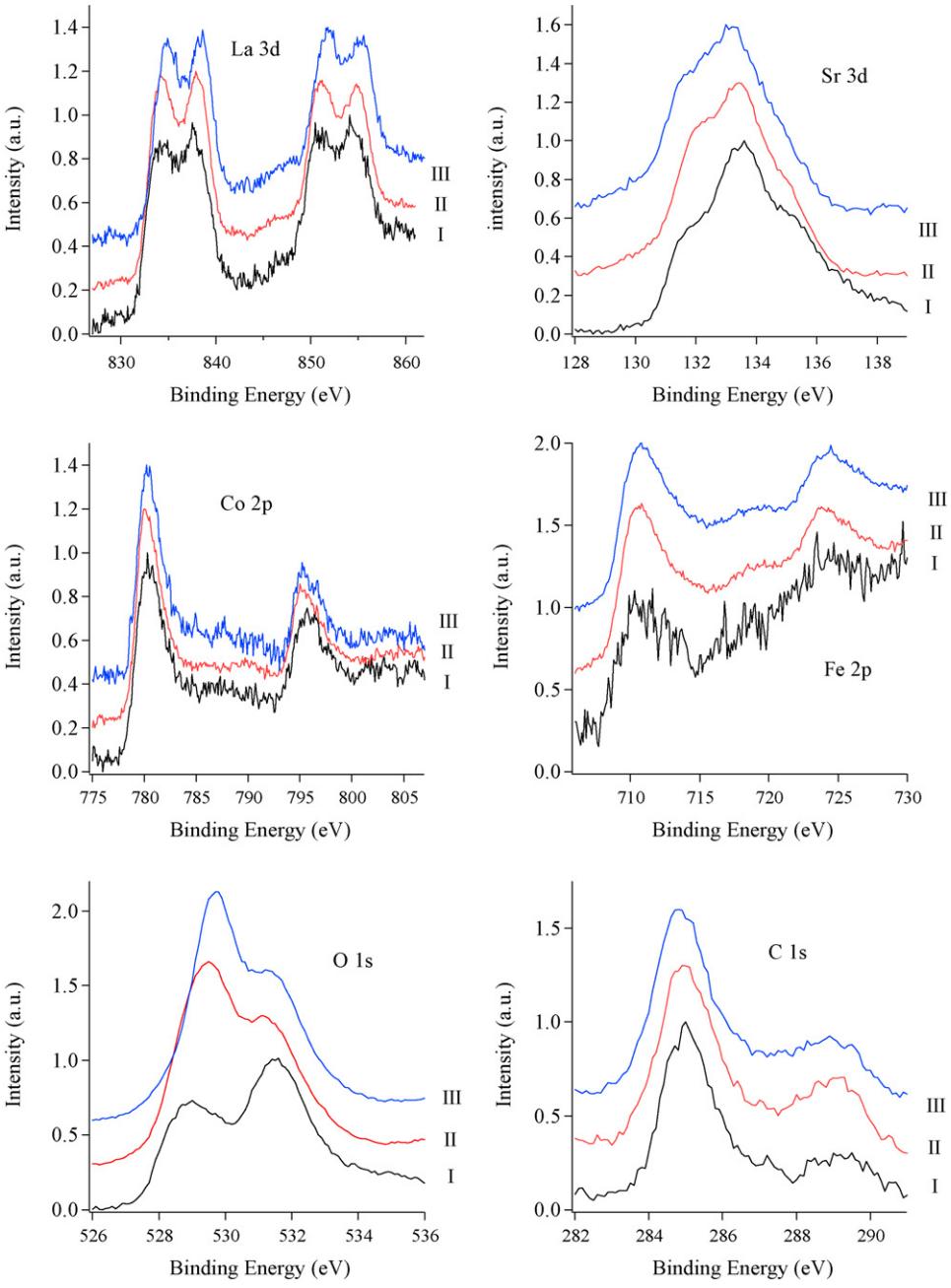

Fig. 2. La 3d, Sr 3d, Co 2p, Fe 2p, O 1s, C 1s XP spectra obtained for the LSCF and Fe_2O_3/LSCF powder samples. LSCF (I), Fe_2O_3/LSCF supported samples 1:9 (II) and 1:1 (III). The spectra of La 3d, Sr 3d, Co 2p and C 1s are normalized with respect to their maximum value while O 1s and Fe 2p XP spectra are normalized with respect to the peaks at 531.4 and 711.0 eV, respectively.

The involvement of the perovskite oxygen in the products formation is consistent with the abrupt activity drop observed.

The Boudouard reaction however (Eq. (2)), should be favored at high temperature [17] whereas, at lower temperature, an important role can be played by oxygen. Two different reaction mechanisms have been proposed for perovskites oxidation reactions, involving two different oxygen species [40,41]: at low temperature the interaction between adsorbed oxygen and reactants is assumed. At high temperature, when the coverage of molecular O_2 strongly decreases, lattice oxygen becomes active. From TPD investigations two kinds of oxygen were revealed in literature [40,41]: the first one, indicated as α-oxygen, is considered to desorb from the surface of the solid (as O^- or O^{2-}); the second one, β-oxygen, is supposed to originate from the bulk of the solid (as O^{2-}) with the simultaneous reduction of Co^{3+} to Co^{2+}. Consistently, the oxidation reaction mechanisms have been interpreted considering α- and β-oxygen: for low-temperature reactions (such as CO oxidation) a suprafacial mechanism with the participation of surface oxygen is suggested whereas for high temperature reactions an intrafacial mechanism involving lattice oxygen is preferred. More recent investigations suggest an active role of grain boundaries and a possible desorption of β-oxygen due to the reduction of grain boundaries segregated Co^{3+} [42].

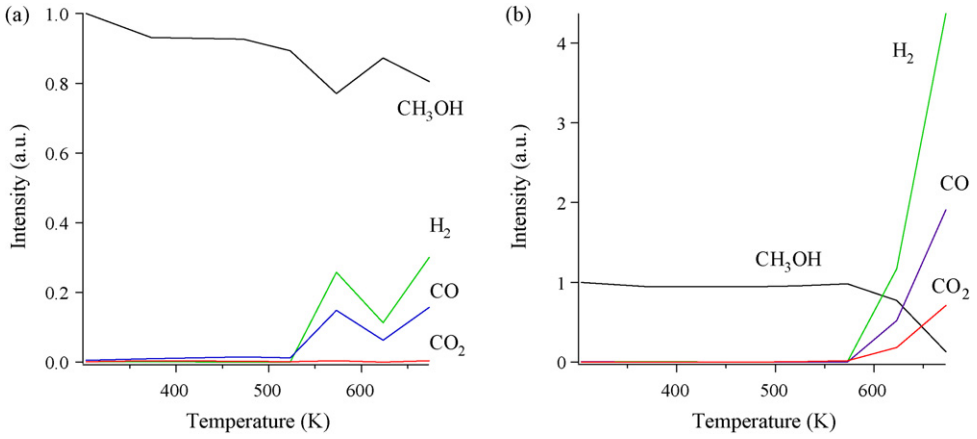

Fig. 3. QMS data obtained, as a function of temperature for the interaction of LSCF with (a) methanol and (b) 1 M methanol solution: (—) CH_3OH, (▬) H_2, (▬) CO and (▬) CO_2.

To test this hypothesis a re-activation treatment with oxygen (carried out flowing oxygen 100% at 673 K for 1 h, flow rate 50 cm^3/min) was performed on the nano-catalyst exposed to methanol at 673 K. After this treatment the interaction with methanol was newly investigated (Fig. 5, black line): in this case the intensity of the QMS signal attributed to CO_2 greatly increases particularly at the beginning, and the CO and H_2 formation is also favored thus indicating a role of weakly bound oxygen species in methanol oxidation. As a general consideration the activity of lanthanide perovskites was observed to depend mainly on the nature of the transition metal [1]; dopants (such as Sr, in the present case) can also influence the Co^{3+}/Co^{2+} presence and thus the activity in oxidation reactions. Co^{3+} sites, in particular, are considered to be the active sites for CO oxidation in cobalt containing oxides through the CO coordination [43,44].

3.2.2. LSCF: interaction with methanol 1 M

When a 1 M solution of methanol in de-ionized water was used instead of pure methanol, the activity of the catalyst (Figs. 3b and 4b) starts at about 623 K (instead of 573 K) and increases with temperature with a more regular trend.

At 623 K the CO and H_2 formation starts after ca. 180 s and reaches a stable value around 800 s (Fig. 6). Unlike the case of pure methanol, CO_2 formation is evidenced both from the QMS and IR data (Figs. 4b and 6); moreover the intensity of the corresponding signal is maximum after 180 s and then decreases until about 400 s (growing then slowly for increasing time). At 673 K the reaction begins immediately and a greater activity is observed; a stable situation is reached in 300–350 s. CO_2 formation growths with time aiming to reach a plateau value after ca. 1050 s.

The relevant formation of carbon dioxide suggests that steam-reforming reaction takes place:

$$CH_3OH + H_2O \rightleftarrows CO_2 + 3H_2 \quad (4)$$

The steam-reforming reaction is often explained as the sum of methanol decomposition (1) and water gas shift reaction (5) [16,17]:

$$CO + H_2O \rightleftarrows CO_2 + H_2 \quad (5)$$

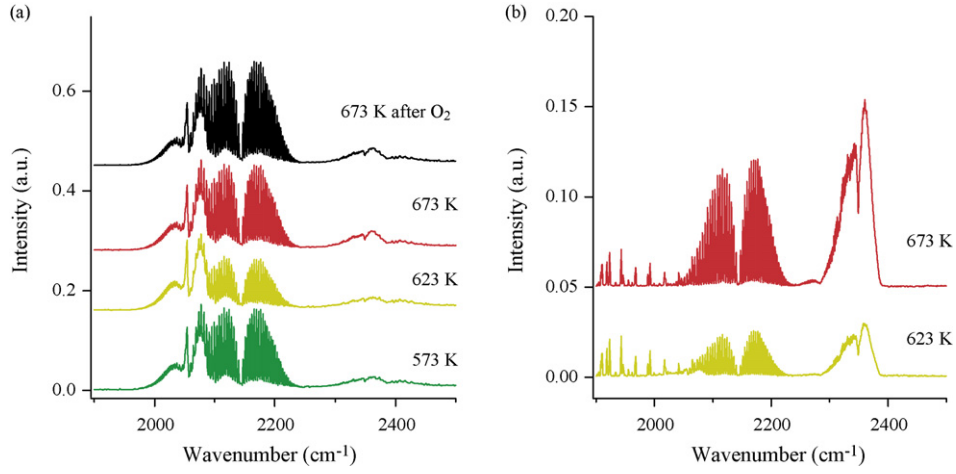

Fig. 4. IR spectra of the reaction products for the interaction of LSCF with (a) methanol and (b) 1 M methanol solution; region between 1900 and 2500 cm^{-1}.

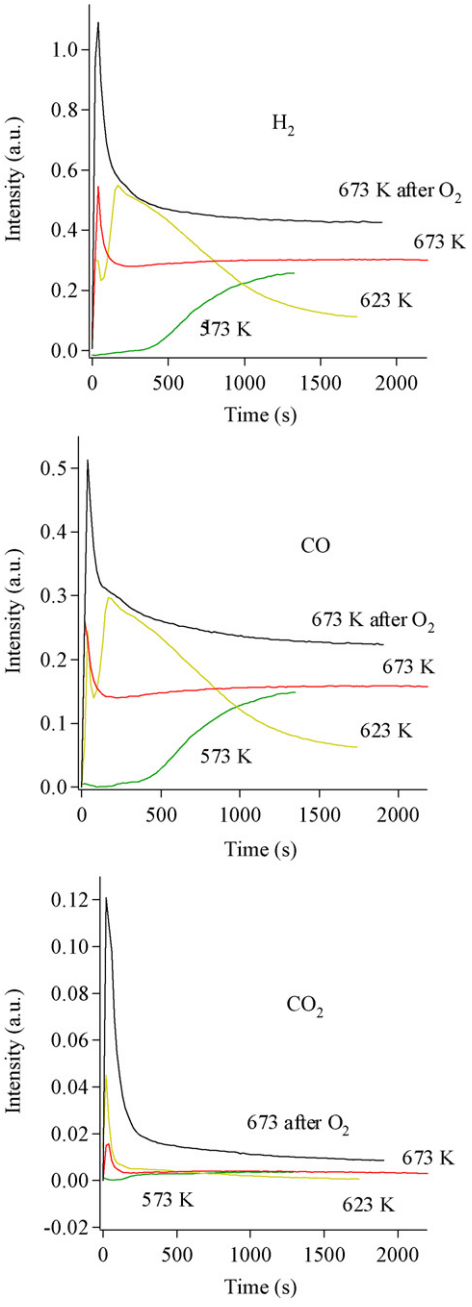

Fig. 5. QMS data (concerning H_2, CO and CO_2) obtained as a function of time and temperature for the interaction of LSCF with methanol: (▬) 573 K, (▬) 623 K, (▬) 673 K and (—) 673 K after re-activation in pure O_2 flow at 673 K.

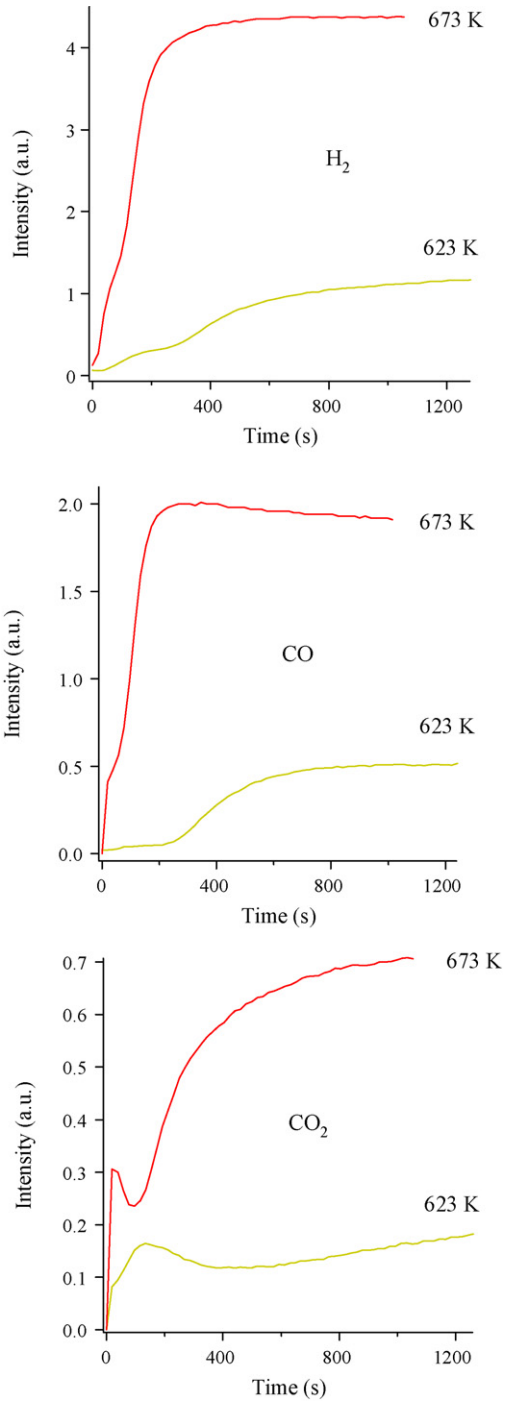

Fig. 6. QMS data (concerning H_2, CO and CO_2) obtained as a function of time and temperature for the interaction of LSCF with 1 M methanol solution: (▬) 623 K and (▬) 673 K.

A decomposition through methyl formate decomposition is also suggested [45]:

$$2CH_3OH \rightleftarrows HCOOCH_3 + 2H_2 \quad (6)$$

$$HCOOCH_3 + H_2O \rightleftarrows HCOOH + CH_3OH \quad (7)$$

$$HCOOH \rightleftarrows CO_2 + H_2 \quad (8)$$

In the present case, however, methyl formate and formic acid were never observed.

Lwin et al. [15] carried out a thermodynamic study showing that the equilibrium concentrations of formic acid and/or methyl formate are zero and suggesting thus that if these components are involved in the reaction path they are merely intermediates. The thermodynamic model also indicates that dimethyl ether formation is favored at low temperatures and low steam/carbon feed ratios whereas carbon monoxide occurs at high temperatures and low steam carbon ratios (intermediate conditions can minimize the formation of both these by-products). Methanol conversion and selectivity for

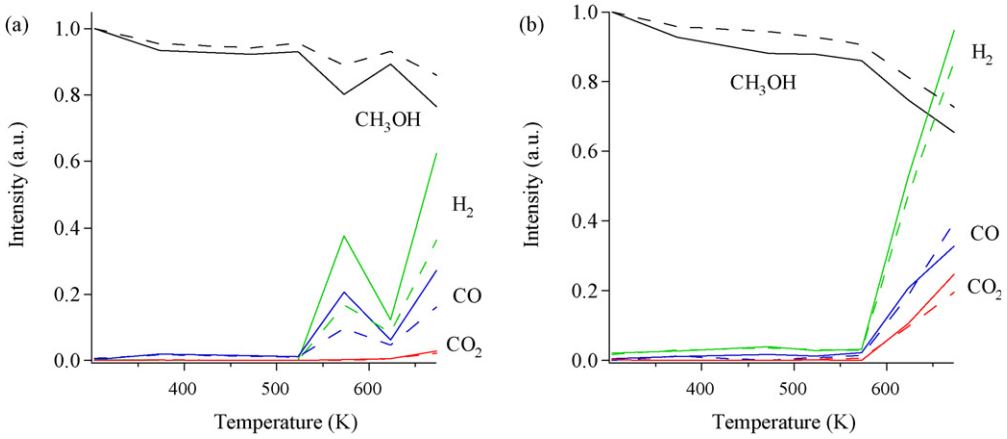

Fig. 7. QMS data obtained as a function of temperature for the interaction of Fe_2O_3/LSCF 1:9 (solid line) and 1:1 (dashed line) with (a) methanol and (b) 1 M methanol solution: (—) CH_3OH, (▬) H_2, (▬) CO and (▬) CO_2.

hydrogen result to be higher when water is present; Peppley et al. also reported that methanol decomposition is much slower than the steam-reforming methanol reaction [46].

The results, reported in Fig. 6, suggest two steps in the reaction: during the first one the main products are carbon dioxide and hydrogen whereas carbon monoxide and hydrogen are prevalent in the second step. This is particularly evident when the reaction is carried out at 623 K: in this case the first step starts immediately and stops after about 350 s. At 673 K the first step lasts only few tenths of seconds. These results are consistent with a prevalent formation of CO for increasing reaction time and lower

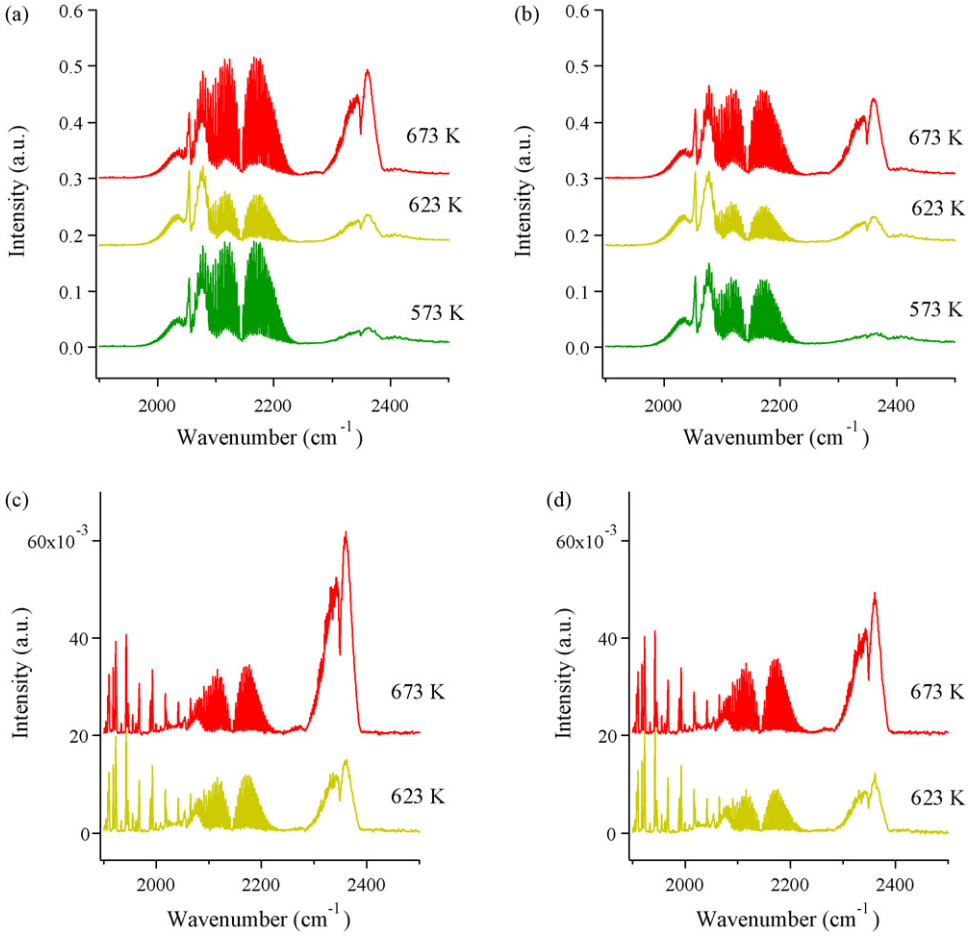

Fig. 8. IR spectra of the reaction products for the interaction of Fe_2O_3/LSCF (a) 1:9 and (b) 1:1 with methanol and (c) 1:9 and (d) 1:1 with 1 M methanol solution; region between 1900 and 2500 cm^{-1}.

temperatures while carbon dioxide is favoured at higher temperatures.

Patel et al. [16] during their investigation of the oxidative steam reforming of methanol observed that CO formation increases with contact time increment as a consequence of the reverse water gas shift reaction (rWGS):

$$H_2 + CO_2 \rightleftarrows H_2O + CO \quad (9)$$

In the present case the concomitant increase of hydrogen and carbon monoxide could be indicative of the methanol decomposition (Eq. (1)).

3.2.3. Fe_2O_3/LSCF: interaction with methanol

QMS and IR data show, for the nanocomposite catalysts, the same trend in activity observed for the supporting nanoscale LSCF (Figs. 7a and 8a and b) thus suggesting a similar reaction mechanism. Beside H_2, the only observed products, as confirmed by IR spectra (Fig. 8a and b), are CO, and CO_2. The comparison with the results obtained for LSCF reveals a slightly higher reactivity for the sample with lower iron content while no significant differences can be observed between LSCF and Fe_2O_3/LSCF 1:1 wt. As already observed for LSCF, at 573 K the reaction starts after 500 s (Fe_2O_3/LSCF 1:9 wt.) and 900 s (Fe_2O_3/LSCF 1:1 wt.) after 1500 s (Fe_2O_3/LSCF 1:9 wt.) and 1800 s (Fe_2O_3/LSCF 1:1 wt.) (Fig. 9) a rather stable situation is going to be reached. At 623 the reaction begins immediately but the activity rapidly decreases and the stable situation is reached in few minutes; the lower reactivity is also confirmed by IR results (Fig. 8a and b). A marked increment of reactivity is observed at 673 K, moreover a stable situation is reached immediately. Noteworthy, at 673 K the formation of carbon dioxide is rather significant (Figs. 8a and b and Fig. 9) suggesting a different reactivity of the nanocomposite catalysts with respect to the supporting nanosized LSCF.

3.2.4. Fe_2O_3/LSCF: interaction with methanol 1 M

Like in the case of LSCF, when a 1 M solution of methanol in de-ionized water is used as feed the activity of the nanocatalysts (Figs. 7b and 8c and d) increases with temperature with a monotone trend. As a general consideration the comparison with the QMS and IR results obtained for LSCF clearly indicates a decreased reactivity; this can be evidenced by comparing Figs. 3b with 7b and 4b with 8c and d. It is interesting to note that Nitadori et al. observed a strong decrease of the catalytic activity for propane oxidation when using an iron containing perovskite thus suggesting the central role played by the transition metal in the reactivity of a perovskite [47]. The obtained results are consistent with a higher activity of the nanocomposite catalyst with lower iron content (Fe_2O_3/LSCF 1:9 wt.).

At 623 K CO formation starts after about 500 s (Fig. 10) with Fe_2O_3/LSCF 1:9 wt. as catalyst and after 600–700 s with Fe_2O_3/LSCF 1:1 wt. (in this case CO raises up slowly for the firsts 1200 s, then a more evident growth is noted). H_2 trend is equally significant; the formation of H_2 begins immediately and slowly increases until 480 s (Fe_2O_3/LSCF 1:9 wt.), 1200 s (Fe_2O_3/LSCF 1:1 wt.) then a marked increment is observed.

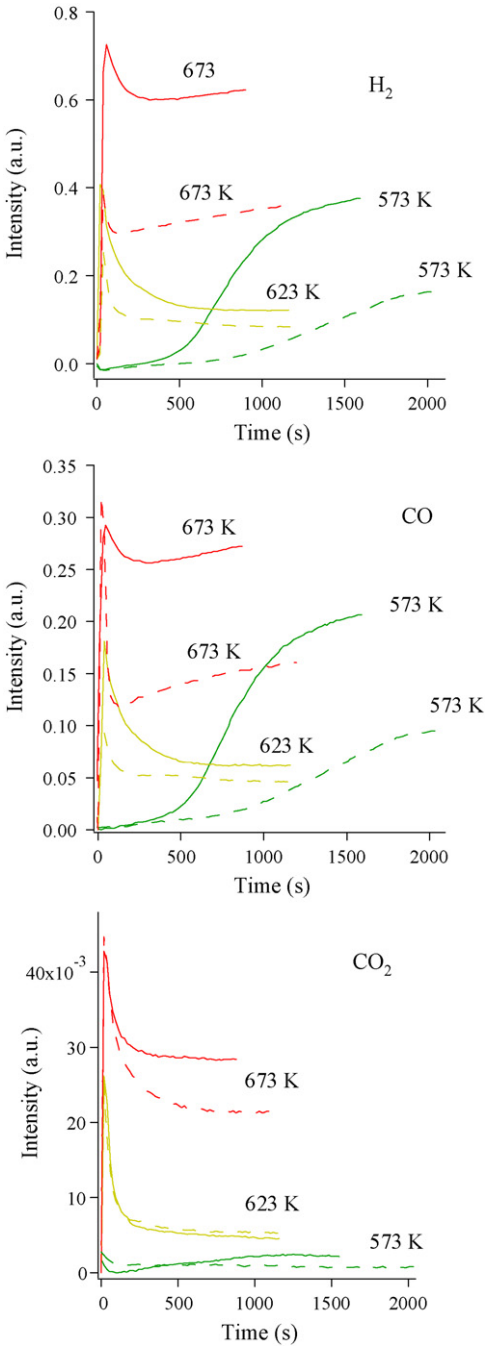

Fig. 9. QMS data (concerning H_2, CO and CO_2) obtained as a function of time and temperature for the interaction of Fe_2O_3/LSCF 1:9 (solid line) and 1:1 (dashed line) with methanol: (▬) 573 K, (▬) 623 K and (▬) 673 K.

These observations suggest that, at 623 K, the overall steam reforming is the main reaction occurring in the beginning. At increasing time, the rate of steam reforming seems rather constant while the methanol decomposition becomes faster producing increasing amounts of H_2 and CO. At 673 K both the reactions begin immediately and after 1000–1200 s a stable situation is reached.

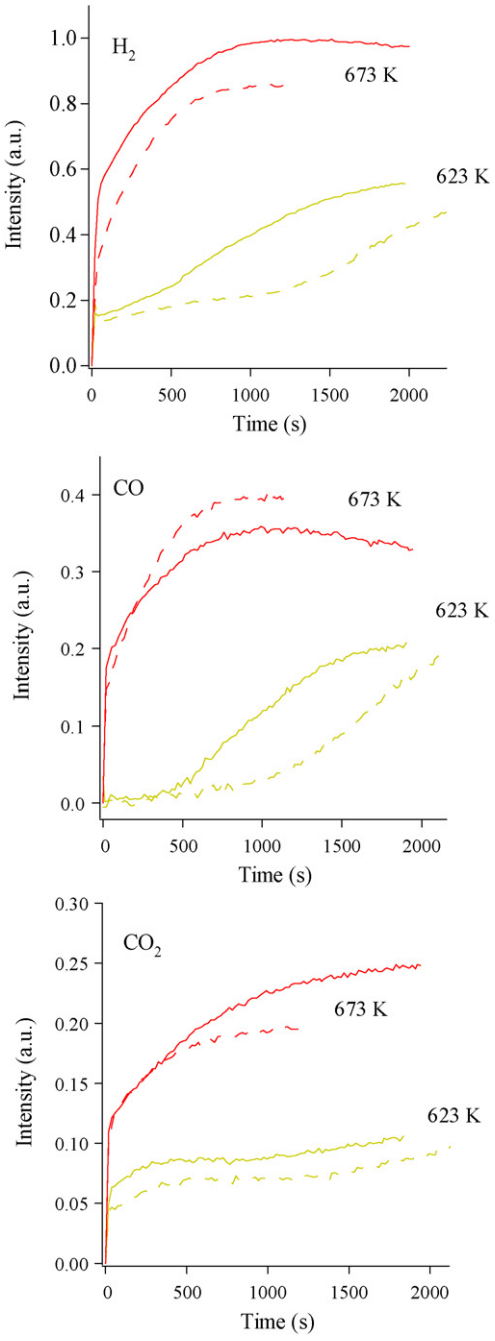

Fig. 10. QMS data (concerning H_2, CO and CO_2) obtained as a function of time and temperature for the interaction of Fe_2O_3/LSCF 1:9 (solid line) and 1:1 (dashed line) with 1 M methanol solution: ( ) 623 K and ( ) 673 K.

The comparison between the QMS and IR data obtained with and without steam suggests that in the absence of steam, methanol mainly decomposes whereas methanol deep oxidation can be due to surface oxygen species [48]. When steam is present in the reactive mixture steam-reforming reaction and methanol decomposition are both observed and the prevailing reaction path is strongly influenced by the sample composition and the reaction conditions.

4. Conclusions

In this paper a perovskite-type oxide ($La_{0.6}Sr_{0.4}Co_{0.8}Fe_{0.2}O_{3-\delta}$) is prepared by Pechini method; two Fe_2O_3/LSCF nanocomposites characterized by a different iron oxide content (Fe_2O_3/LSCF = 1:9 and 1:1 wt.) are obtained by impregnation.

XRD pattern of LSCF shows, beside the desired perovskite phase, $SrLaCoO_4$ and traces of La_2O_3 and Co_3O_4. In the XRD patterns of the supported samples several crystallographic phases appear as a consequence of the iron oxide deposition: $Sr_{0.4}Fe_{0.6}La_{0.6}Co_{0.4}O_3$ and $SrCO_3$ in the sample Fe_2O_3/LSCF = 1:9; Fe_2O_3, $SrLaFeO_4$, and traces of iron rich phases, in the sample Fe_2O_3/LSCF = 1:1.

The reactivity of the obtained samples with respect to pure methanol and to a 1 M aqueous solution of methanol was investigated by QMS and IR spectroscopy. When only methanol is present the main reaction is the alcohol decomposition to CO and H_2 whereas steam reforming is observed at $T \geq 673$ K with the 1 M methanol solution. The reactivity was investigated as a function of time and the influence of temperature, sample composition and reactive mixture was revealed.

Acknowledgments

The authors gratefully acknowledge Professor E. Tondello for helpful discussions. This work was supported by research programs: FISR-MIUR “Nanosistemi inorganici ed ibridi per lo sviluppo e l’innovazione di celle a combustibile” and Progetto di ateneo—2004 “Nuovi sistemi nanocompositi come materiali attivi in celle a combustibile ad ossido solido”.

References

[1] M.A. Pena, J.L.G. Fierro, Chem. Rev. 101 (2001) 1981.
[2] S.M. Haile, Acta Mater. 51 (2003) 5981.
[3] A. Galenda, M.M. Natile, V. Krishnan, H. Bertagnolli, A. Glisenti, Chem. Mater. 19 (2007) 2796.
[4] A. Mineshige, J. Izutsu, M. Nakamura, K. Nigaki, J. Abe, M. Kobune, F. Satoshi, T. Yazawa, Solid State Ionics 176 (2005) 1145.
[5] M. Weston, I.S. Metcalfe, D. Mantzavinos, Catal. Today 55 (2000) 197.
[6] S.J. Xu, W.J. Thomson, Ind. Eng. Chem. Res. 37 (1998) 1290.
[7] L.-W. Tai, M.M. Nasrallah, H.U. Anderson, D.M. Sparlin, S.R. Sehlin, Solid State Ionics 76 (1995) 259–271.
[8] Q. Xu, D.-P. Huang, W. Chen, J.-H. Lee, H. Wang, R.-Z. Yuan, Scr. Mater. 50 (2004) 165.
[9] A. Glisenti, G. Favero, G. Granozzi, J. Chem. Soc., Faraday Trans. 94 (1998) 173.
[10] M.P. Pechini, U.S. Patent 3,330,697 (1967).
[11] A.C. Tas, P.J. Majewski, F. Aldinger, J. Am. Ceram. Soc. 83 (2000) 2954.
[12] D. Segal, In: R.W. Cahn, P. Haasen, E.J. Kramer (Eds.), Material Science and Technology: A Comprehensive Treatment, vol. 17A: Processing of ceramics (Chapter 3, and references therein, R.J. Brook (Ed.)), 1996.
[13] J.A. Schwarz, C. Contescu, A. Contescu, Chem. Rev. 95 (1995) 477.
[14] H.H. Kung, Transition Metal Oxides: Surface Chemistry and Catalysis, Elsevier, 1989.
[15] Y. Lwin, W. Ramli, W. Daud, A.B. Mohamad, Z. Yaakob, Int. J. Hydrogen Energy 25 (2000) 47.
[16] S. Patel, K.K. Pant, Chem. Eng. Sci. 62 (2007) 5436.
[17] N. Laosiripojana, S. Assabumrungrat, Chem. Eng. Sci. 61 (2006) 2540.

[18] T. Nishiguchi, T. Matsumoto, H. Kanai, K. Utani, Y. Matsumura, W.-J. Shen, S. Imamura, Appl. Catal. A: Gen. 279 (2005) 273.
[19] P. Biswas, D. Kunzru, Int. J. Hydrogen Energy 32 (2007) 969.
[20] D.A. Shirley, Phys. Rev. B 5 (1972) 4709.
[21] J.F. Moulder, W.F. Stickle, P.E. Sobol, K.D. Bomben, in: J. Chastain (Ed.), Handbook of X-ray Photoelectron Spectroscopy, Physical Electronics, Eden Prairie, MN, 1992.
[22] D. Briggs, J.C. Riviere, in: D. Briggs, M.P. Seah (Eds.), Practical Surface Analysis, Wiley, New York, 1983.
[23] S.G. Lias, S.E. Stein, NIST/EPA/MSDC Mass Spectral Database PC version 3.0, June 1990.
[24] The peak at *m/e* 28 remaining after subtraction of the contributions of methanol and formaldehyde was attributed to CO (incidentally the presence of air contamination was never observed in the HV chamber); the signal at *m/e* 44 was assigned at carbon dioxide whereas the contributions at 29 *m/e* were attributed to methanol. Hydrogen formation was estimated by means of the peak at *m/e* 2.
[25] JCPDS Cards: $La_{0.6}Sr_{0.4}Co_{0.8}Fe_{0.2}O_3$ = 48-0124, La_2O_3 = 74-1144, Co_3O_4 = 42-1467, $La_{2-x}Sr_xCoO_4$ = 83-2412, $Sr_{0.4}Fe_{0.6}La_{0.6}Co_{0.4}O_3$ = 49-0284, $SrCO_3$ = 74-1491, Fe_2O_3 = 84-0308, $Fe_{2.94}O_4$ = 86-1355 $Sr_4Fe_3O_{10-x}$ = 22-1429, $FeLaO_3$ = 37-1493 $LaCoO_3$ = 86-1664.
[26] H.P. Klug, L.E. Alexander, X-Ray Diffraction Procedures For Polycrystalline and Amorphous Materials, 2nd ed., John Wiley & Sons, 1974.
[27] M. Machkova, N. Braskova, P. Ivanov, J.B. Carda, V. Kozhukharov, Appl. Surf. Sci. 119 (1997) 127.
[28] V. Kozhukharov, M. Machkova, P. Ivanov, H.J.M. Bouwmeester, R.J. Van Doorn, Mater. Sci. Lett. 15 (1996) 1727.
[29] A.E. Bocquet, P. Chalcker, J.F. Dobson, P.C. Healy, S. Myhra, J.G. Thompson, Phys. C 160 (1989) 252.
[30] NIST Standard Reference Database 20, Version 3.4.
[31] K. Tabata, S.J. Kohiki, Mater. Sci. Lett. 6 (1987) 1030.
[32] Co(II) and Co(III) oxides can be differentiated in XPS using their different magnetic properties. As a matter of fact the XP spectra of Co(II) high spin compounds, such as CoO, are characterized by an intense shake-up satellite structure around 787.0 eV and 804.0 eV. Unlike Co(II) compounds, in the low spin Co(III) compounds the satellite structure is weak or missing. Co_3O_4, a mixed valence oxide, shows a weak satellite structure symptomatic of shake-up from the minor Co(II) component. See, as an example, N.S. McIntyre, M.G. Cook, Anal. Chem., 47 (1975) 2208.
[33] M.M. Natile, A. Glisenti, Chem. Mater. 14 (2002) 3090.
[34] A. Galenda, M.M. Natile, A. Glisenti, Surf. Sci. Spectra 13 (2006) 32 (and references therein).
[35] M.I. Solsulnikow, Y.A. Teterin, J. Electron. Spectrosc. Relat. Phenom. 59 (1992) 111.
[36] P.A.W. van der Heide, Surf. Interface Anal. 33 (2002) 414.
[37] A.E. Bocquet, H. Namatame, A. Fujimori, Y. Takeda, M. Takano, Surf. Sci. Spectra 6 (1999) 294.
[38] S.N. Shkerin, M.V. Kuznetsov, N.A. Kalashnikova, Russ. J. Electrochem. 39 (2003) 591.
[39] M. Imamura, N. Matsubayashi, H. Shimada, J. Phys. Chem. B 104 (2000) 7348.
[40] S. Royer, F. Bérubé, S. Kaliaguine, Appl. Catal. A: Gen. 282 (2005) 273 (and references therein).
[41] L. Lisi, G. Bagnasco, P. Ciambelli, S. De Rossi, P. Porta, G. Russo, M. Turco, J. Solid State Chem. 146 (1999) 176.
[42] S. Royer, D. Duprez, S. Kaliaguine, J. Catal. 234 (2005) 364 (and references therein).
[43] L. Forni, C. Oliva, F.P. Vatti, M.A. Kandala, A.M. Ezerets, A.V. Vishniakov, Appl. Catal. B: Environ. 7 (1996) 269 (and references therein).
[44] F. Grillo, M.M. Natile, A. Glisenti, Appl. Catal. B: Environ. 48 (2004) 267 (and references therein).
[45] C.J. Jiang, D.L. Trimm, M.S. Wainwright, N.W. Cant, Appl. Catal. A: Gen. 97 (1993) 145.
[46] B.A. Peppley, J.C. Amphlett, L.M. Kearns, R.F. Mann, Appl. Catal. A: Gen. 179 (1999) 31.
[47] T. Nitadori, I. Tatsumi, M. Misono, Bull. Chem. Soc. Jpn. 61 (1988) 621.
[48] L.A. Isupova, I.S. Yakovleva, G.M. Mlikina, V.A. Rogov, V.A. Sadykov, Kinet. Catal. 46 (2005) 729.